UC San Diego
UC San Diego Previously Published Works

Title

T-Cell-Mimicking Nanoparticles Can Neutralize HIV Infectivity.

Permalink

https://escholarship.org/uc/item/30k4r9ct

Journal

Advanced Materials, 30(45)

Authors

Wei, Xiaoli
Zhang, Gang
Ran, Danni
et al.

Publication Date

2018-11-01

DOI

10.1002/adma.201802233

Peer reviewed

T-Cell-Mimicking Nanoparticles Can Neutralize HIV Infectivity

Xiaoli Wei

Department of NanoEngineering and Moores Cancer Center University of California San Diego La Jolla, CA 92093, USA

Gang Zhang

Division of Infectious Diseases Department of Pediatrics University of California San Diego La Jolla, CA 92093, USA

Danni Ran, **Nishta Krishnan**, **Ronnie H. Fang**, and **Weiwei Gao**

Department of NanoEngineering and Moores Cancer Center University of California San Diego La Jolla, CA 92093, USA

Stephen A. Spector

Division of Infectious Diseases Department of Pediatrics University of California San Diego La Jolla, CA 92093, USA

Liangfang Zhang

Department of NanoEngineering and Moores Cancer Center University of California San Diego La Jolla, CA 92093, USA

Abstract

To improve human immunodeficiency virus (HIV) treatment and prevention, therapeutic strategies that can provide effective and broad-spectrum neutralization against viral infection are highly desirable. Inspired by recent advances of cell-membrane coating technology, herein, plasma membranes of CD4$^+$ T cells are collected and coated onto polymeric cores. The resulting T-cell-membrane-coated nanoparticles (denoted as "TNPs") inherit T cell surface antigens critical for HIV binding, such as CD4 receptor and CCR5 or CXCR4 coreceptors. The TNPs act as decoys for viral attack and neutralize HIV by diverting the viruses away from their intended host targets. This decoy strategy, which simulates host cell functions for viral neutralization rather than directly suppressing viral replication machinery, has the potential to overcome HIV genetic diversity while not eliciting high selective pressure. In this study, it is demonstrated that TNPs selectively bind with gp120, a key envelope glycoprotein of HIV, and inhibit gp120-induced killing of bystander CD4$^+$ T cells. Furthermore, when added to HIV viruses, TNPs effectively neutralize the viral infection of peripheral mononuclear blood cells and human-monocyte-derived macrophages in a dose-dependent manner. Overall, by leveraging natural T cell functions, TNPs show great potential as a new therapeutic agent against HIV infection.

Keywords

antiretroviral therapy; biomimetic nanoparticle; cell membrane coating; HIV; T cell; viral neutralization

---

Despite recent therapeutic advances, human immunodeficiency virus (HIV) type-1 infection remains incurable.[1,2] Although combination antiretroviral therapy is effective in controlling plasma virus at an undetectable level, HIV persists in reservoir cells.[3,4] Residual viruses that escape from the treatment maintain active viral replication in latent cells, posing a major obstacle for viral eradication.[5] Current antiretroviral therapy must be taken for a lifetime. Discontinuation of treatment results in rapid viral rebound within days or weeks.[6,7] In addition, adverse effects and emergence of drug resistance further challenge the therapeutic outcome of conventional drug therapies.[8,9] To address these challenges, broadly neutralizing antibodies that target HIV envelope glycoproteins of the circulating HIV virions have received much attention.[10,11] However, as the immunity generated by these antibodies remains low, neutralization against cell free viruses is inefficient and the treatment outcome remains unsatisfactory.[12] Mean-while, enormous efforts have been devoted to developing safe and effective vaccines as preventive strategies against HIV infection.[13] However, so far no HIV envelope (Env) immunogen has been identified to elicit antibodies with broadly neutralizing activity.[14] Apparently, the absence of curative treatment or vaccines underscores a great need for innovative therapeutic approaches against HIV infection.

The rapid development of nanotechnology has recently led to therapeutic nanoparticles tailored to improve the treatment and prevention of HIV infection.[15–17] For example, nanoparticles have been used as delivery vehicles for antiviral drugs to improve drug tolerability, circulation half-life, and efficacy.[18] Various nano-particles have also been found to directly interfere with and inhibit viral replication through mechanisms such as multi-valent presentation of small molecules and direct blockage of viral assembly processes.[19,20] Nanoparticles have also enabled nonviral delivery of small interfering RNAs (siRNAs) to silence gene expression in repertoire cells (such as CD4$^+$ lymphocytes, macrophages, and dendritic cells) and HIV viruses.[21,22] Mean-while, nanoparticle-based vaccine strategies also offer high capabilities of modulating host immune responses through improved immune targeting and combined presentation of antigen and adjuvant, which together enhance vaccine safety and anti-HIV immunity.[16]

As therapeutic nanoparticles are gaining traction for HIV treatment and prevention, cell-membrane-coated nanoparticles recently emerged as a unique biomimetic platform to treat various human diseases.[23,24] These nanoparticles are made by wrapping plasma membranes of natural cells onto synthetic cores and therefore are capable of mimicking source cells for bioactivity. One application of cell-membrane-coated nanoparticles is to act as decoys of susceptible cells to intercept and neutralize pathologic agents. Particularly, nano-particles coated with a red blood cell membrane (RBC-NPs) have demonstrated robust capability of neutralizing bacterial pore-forming toxins, pathological autoantibodies, and nerve agents.[25–27] Similarly, nanoparticles coated with the membrane of macrophages were able to neutralize endotoxins and proinflammatory cytokines, which together reduced

lethality of sepsis in mice.[28] Following the initial development, nanoparticles coated with membranes of various cell types including cancer cells, platelets, leukocytes, stem cells, and bacteria have all been successfully developed, offering numerous therapeutic opportunities through cell-mimicking properties and multifaceted biointerfacing.[24]

The unique biomimicry of cell-membrane-coated nanoparticles intrigued us to develop this technology for potential anti-HIV treatment. Depletion of immune cells is the hallmark of HIV infection, leading to acquired immunodeficiency syndrome (AIDS) and increased risk of opportunistic infections as well as cancers.[29] In particular, infection leads to the depletion of $CD4^+$ T helper cells through different mechanisms, such as direct viral killing of infected cells, killing by HIV-specific cytotoxic T cells, or apoptosis of uninfected bystander cells. The virus entry/fusion is initiated by the interaction between viral envelope glycoproteins, mainly gp120, and cluster of differentiation 4 (CD4) receptor, followed by binding to C–C chemokine receptor type 5 (CCR5) or C-X-C chemokine receptor type 4 (CXCR4) coreceptors on the target cells.[3] Based on this mechanism, herein, we derived plasma membrane of natural $CD4^+$ T lymphocyte cells and fused it onto polymeric cores (Figure 1). The resulting T-cell-membrane-coated nanoparticles (denoted as TNPs) mimic parent T cells to target and bind with the viruses. We hypothesize that TNPs inherit the natural adhesion of $CD4^+$ T cells toward HIV and subsequently neutralize HIV infectivity by diverting viral attack away from the host cells. In the study, we confirmed the selective binding of TNPs with viral glycoprotein gp120. We also showed that such binding activity led to the inhibition of gp120-induced killing of bystander T cells in vitro. We further used R5 viruses and X4 viruses, two strains of HIV that exploit CCR5 or CXCR4 coreceptor for entry and demonstrated the efficacy of TNPs in inhibiting HIV infection of peripheral blood mononuclear cells (PBMCs) in vitro. Overall, this study demonstrates the therapeutic potential of TNPs as a new nanotherapeutic approach against HIV infection.

The formulation of TNPs is a three-step process based on a previously developed method. [30] In the first step, cytoplasm membrane of SUP-T1 cells, a human T lymphoblast cell line, was derived with combined hypotonic lysis, mechanical disruption, and differential centrifugation. In the second step, polymeric cores of poly(lactic-co-glycolic acid) (PLGA) were synthesized with a nanoprecipitation method by adding the polymer in organic solvent to an aqueous phase followed by evaporation. In the third step, cell membrane was fused onto PLGA cores by mixing the two components followed by sonication. Dynamic light scattering (DLS) measurements showed that upon cell membrane coating, the diameter of the nanoparticles increased from 88.3 ± 1.3 to 105.4 ± 4.4 nm and the surface zeta potential increased from -49.2 ± 1.0 to -29.5 ± 1.2 mV (Figure 2a). An increase of ≈17 nm of diameter and 20 mV of surface zeta potential is consistent with the addition of a bilayer membrane onto the exterior of the polymeric core. When examined under transmission electron microscopy (TEM), the resulting TNPs showed a typical core−shell structure depicting unilamellar membrane coating around the core (Figure 2b). Following the formulation, TNPs were suspended in 1× PBS or 50% serum and monitored by DLS for 72 h. Under both conditions, TNPs maintained stable sizes, indicating a high colloidal stability attributable to membrane coating (Figure 2c). Overall, these results indicate the successful coating of polymeric cores with T cell membrane.

Following the physicochemical characterizations of TNPs, surface proteins of TNPs were examined to verify T cell functionalization. First, protein profiles of T cell lysate, T-cell-membrane-derived vesicles (T vesicles), and TNPs were analyzed with sodium dodecyl sulfate polyacrylamide gel electrophoresis (SDS-PAGE). As shown in Figure 3a, the protein profile of TNPs was modulated when compared to T cell lysate (including intracellular proteins) but matched well with that of T vesicles (without intracellular proteins), indicating the preservation of membrane proteins on TNPs throughout the fabrication process. In addition, Western blotting analysis was performed to examine viral receptors related to HIV entry, including CD4 receptor, CCR5 coreceptor, and CXCR4 coreceptor. All three receptors were confirmed in T cell lysate, T vesicles, and TNPs (Figure 3b). A significant enrichment was observed in T vesicles and TNPs, further confirming the translocation of T cell membranes and associated membrane proteins onto nanoparticle surfaces. The cell membrane coating process is driven by the semistable nature of the T vesicles and PLGA cores, during which the asymmetric repulsion between the cores and the extracellular membrane versus the intracellular membrane determines the right-side-out membrane orientation.[31] To confirm such orientation, we stained TNPs and T cells containing equal amounts of membrane content with fluorescence-labeled CCR5 antibodies. After the removal of free antibodies, the TNP sample showed a comparable fluorescence intensity with that of the T cell sample (Figure 3c). As inside-out membrane coating would likely block antibody staining and reduce fluorescence intensity, comparable fluorescence intensity between TNPs and T cells suggests that TNPs adopted primarily a right-side-out membrane orientation.

We next investigated the binding capability and specificity of TNPs to HIV envelope glycoproteins. In the study, recombinant HIV-1 $gp120_{IIIB}$, which represents gp120 of X4 strain, and HIV-1 $gp120_{BaL}$, which represents gp120 of R5 strain, were immobilized onto 96-well plates, respectively. Then fluorescence-labeled TNPs with concentrations ranging from 0.01 to 1.8 mg mL^{-1} were added to the well, followed by incubation and removal of unbound TNPs. It was observed that the fluorescence intensity measured from the captured TNPs increased gradually as TNP concentration increased till it reached a plateau at a TNP concentration of 1 mg mL^{-1} and above (Figure 4a,b). Such two-stage concentration dependence is consistent with previous studies of binding affinity and kinetics of targeted-nanoparticles to ligand-modified 2D surfaces.[32] A Langmuir binary interaction model was used to fit the data curves, leading to a dissociation constant of 0.28 ± 0.06 mg mL^{-1} for immobilized $gp120_{IIIB}$ and a dissolution constant of 0.31 ± 0.05 mg mL^{-1} for $gp120_{BaL}$. To assess whether the binding interaction between TNPs and gp120 was specifically mediated via T cell membrane coating, we also formulated control nanoparticles coated with red blood cell membranes, which have the same core–shell structure and physicochemical properties as TNPs but are functionally inert to HIV, or with synthetic poly(ethylene glycol) (PEG-NPs), which is known to prevent interactions with proteins. Under the same experimental conditions, the gp120-immobolized wells added with RBC-NPs or PEG-NPs showed negligible fluorescence intensity compared to those incubated with TNPs, confirming an active role played by T cell membranes of facilitating nanoparticle-gp120 binding (Figure 4c,d).

After confirming specific binding of TNPs to HIV envelope glycoproteins, we proceeded to evaluate the potential of TNPs for neutralizing the cytotoxicity of gp120. Prior to viral fusion and entry, envelope glycoproteins including gp120 are known to bind to their cellular receptors and chemokine coreceptors, causing bystander CD4$^+$ T cell death.[33] Such apoptosis of uninfected bystander cells has been considered a critical element of HIV pathogenesis as it contributes to the selective depletion of CD4$^+$ T cells, which leads to immunodeficiency. We hypothesize that TNPs can act as T cell decoys to bind with cytopathic gp120 and therefore prevent susceptible T cells from gp120-induced cell death. To test this hypothesis, we first isolated the human PBMCs from healthy donors through density gradient centrifugation. The human CD4$^+$ T cells were purified from isolated PBMCs and verified the purity of at least 95% by flow cytometry. Next, soluble R5-tropic HIV$_{BaL}$ and X4-tropic HIV$_{IIIB}$ gp120 recombinant proteins were premixed with TNPs at 37 °C for 2 h, and further incubated with CD4$^+$ T cells for another 24 h. When treated with HIV$_{BaL}$ gp120 recombinant proteins only, isolated CD4$^+$ T cells showed obvious cell death (Figure 4e). In contrast, cells treated with the mixture of gp120 proteins and TNPs showed significantly reduced apoptosis. When mixed with RBC-NPs or PEG-NPs, gp120 maintained a cytotoxicity level comparable to free protein alone. Such inhibition effect of TNPs was also tested against X4-tropic HIV$_{IIIB}$ gp120 recombinant proteins (Figure 4f). Similar to the previous study, gp120 proteins mixed with RBC-NPs or PEG-NPs induced cell death comparable to gp120 alone. In contrast, cell death decreased significantly when gp120 proteins were mixed with TNPs. These results clearly demonstrate the potential of TNPs to intercept HIV pathogenesis for antiviral activity.

Finally, we proceeded to test whether TNPs binding to HIV envelop glycoprotein can neutralize HIV infection of susceptible host cells. In the study, we chose HIV$_{NL4-3}$ strain and HIV$_{BaL}$ strain that feature distinct cellular tropisms, and first tested their binding interactions with TNPs. The size of HIV$_{NL4-3}$ increased from 120.0 ± 9.5 to 216.7 ± 22.2 nm after incubating with TNPs and that of HIV$_{BaL}$ increased from 131.8 ± 9.4 to 218.4 ± 22.2 nm, implying the complexation between the viruses and TNPs (Figure 5a). Meanwhile, the surface zeta potential of HIV$_{NL4-3}$ decreased from -12.8 ± 1.1 to -23.3 ± 1.3 mV after incubating with TNPs and that of HIV$_{BaL}$ decreased from -14.5 ± 0.9 to -24.3 ± 2.5 nm (Figure 5b).

We next evaluated the neutralization of infectivity by X4 tropic HIV-1$_{NL4-3}$ strain on PBMCs. In this study, 200 TCID$_{50}$ virus was incubated with TNPs ranging from 0 to 3.6 mg mL^{-1} at 37 °C in a 5% CO$_2$ cell culture incubator for 1 h, then added to half million PMBCs and cultured for 48 h. HIV neutralization was quantified by measuring HIV p24 antigen production. After 48 h of incubation, a marked increase in p24 was observed in cultures without TNPs, indicating the occurrence of viral entry and infection of the host cells. However, p24 levels decreased with the increase of TNPs added to the medium, suggesting a dose-dependent neutralization effect (Figure 5c). Based on these results, an IC50 value of 0.49 mg mL^{-1} for TNPs toward inhibiting X4 tropic HIV-1$_{NL4-3}$ strain was obtained by fitting the data with the Hill equation. To further confirm that the inhibition was indeed due to T cell membrane coating, control nanoparticles including RBC-NPs and PEG-NPs, blocking antibodies (a mixture of anti-CCR5, anti-CXCR4, and anti-CD4 antibodies), and TNPs blocked by the antibody mixture were also tested for viral inhibition in comparison

with TNPs. As shown in Figure 5d, PBMCs added with 200 $TCID_{50}$ X4 tropic HIV-1_{NL4-3} viruses showed elevated levels of p24 secretion, but the level remained low when 3.6 mg mL^{-1} TNPs were added to the cell culture. In contrast, RBC-NPs and PEG-NPs added to the cells were unable to reduce p24 secretion. Meanwhile, blocking antibodies added to the host cells were able to inhibit viral infection. When blocked by these antibodies, TNPs showed reduced inhibition against infection, illustrating a direct role played by CD4 and coreceptors on TNPs in diverting viral entry. Cells were also examined for their lactate dehydrogenase (LDH) activity. As shown in Figure 5e, cells treated with PBS, TNPs, RBC-NPs, and PEG-NPs maintained comparable LDH activities, suggesting a negligible toxic effect from nanoparticles alone. The absence of nanoparticle-induced toxicity confirms that the reduced p24 secretion was indeed due to the inhibition of viral entry.

In addition, we performed a similar neutralization assay with R5 tropic HIV-1_{BaL} strain on PMBCs to further test the antiviral activity of TNPs. After 48 h of incubation, a significant p24 secretion level was observed in the sample without TNPs, but decreased with the increase of TNPs premixed with HIV-1_{BaL}, implying a similar dose-dependent inhibitory effect (Figure 5f). In this case, an IC50 value of 0.32 mg mL^{-1} for TNPs toward inhibiting R5 tropic HIV-1_{BaL} strain was obtained. Such HIV infection was inhibited with the addition of TNPs, but not with the control nanoparticle groups. Inhibition was also reduced by blocking TNPs with the antibody mixture. These results together further demonstrate a neutralization and antiviral specificity by T cell membranes (Figure 5g). Similarly, cells in all groups maintained a comparable LDH activity, further confirming that reduction of p24 was indeed due to inhibition of viral entry rather than vehicle-induced cytotoxicity (Figure 5h).

Besides PMBCs, we further assessed whether TNP would prevent HIV infectivity toward other host cells. In particular, HIV internalization by macrophages leads to productive infection and this pathway is known to require CCR5 engagement at the cell surface.[34–36] Therefore, we used HIV-1_{BaL} strain to study whether TNPs can inhibit HIV infection on human-monocyte-derived macrophages (MDMs). After 48 h of incubation of viruses with the cells, p24 secretion level increased significantly in the sample without TNPs, but decreased with the increase of added TNPs, suggesting a dose-dependent inhibitory effect against macrophage infection (Figure 5i). Specifically, an IC50 value of 0.41 mg mL^{-1} for TNPs to inhibit the infection of R5 tropic HIV-1_{BaL} strain to macrophages was derived. Such HIV infection was inhibited with the addition of TNPs, but not with the control nanoparticle groups. Inhibition was also reduced by blocking TNPs with the aforementioned antibody mixture (Figure 5j). Similarly, MDMs in all groups maintained a comparable LDH activity, further confirming that reduction of p24 was indeed due to inhibition of viral entry rather than vehicle-induced cytotoxicity (Figure 5k).

Using cell-mimicking nanoparticles to neutralize viral infectivity is a unique approach against HIV infection, which can potentially become a part of cure strategy for viral infections. Although undetectable in plasma, the replication-competent HIV released from viral reservoirs plays a major role in maintaining latent infection.[5] These viruses escape the suppression of conventional antiretroviral drugs, causing low-level viremia and persistently eliciting new infections. Meanwhile, viral proteins targeted by antiretroviral drugs and

neutralizing antibodies mutate frequently, leading to poor efficacy.[37] In contrast, TNPs mimic natural T cells to bind with HIV for neutralization; therefore their application is less dependent on the prior knowledge of the molecular targets. By leveraging the natural affinity of T cell membrane receptors to HIV, TNPs may overcome the high glycosylation, rapid conformational changes, and steric restriction of the epitopes on HIV envelopes that have limited conventional antibody induction to recognize a broad spectrum of HIV strains. TNP-mediated neutralization also avoids interfering with the molecular pathways of viral replication, therefore likely to pose low pressure for resistance development.

Synthetic nanoparticles have been conjugated with receptor proteins of the host cells to target bacteria or viruses for neutralization.[38,39] While it is promising, conventional "bottom-up" nanoparticle design faces challenges of protein identification and labor-intense chemical synthesis. The fabrication of TNPs bypasses these challenges by exploiting a "top-down" approach that uses natural cell membrane as building materials. Meanwhile, PLGA cores intimately interface with membrane and serve as a solid substrate that restricts membrane fusion and tailors the size of the TNPs.[31] In addition, additional payloads can be encapsulated into PLGA cores or membrane bilayers and combing the TNP technique with other nanotherapeutic approaches, which together may open additional mechanisms of viral suppression.[40–42] By integrating natural cell membrane materials and synthetic nanomaterials, TNPs represent a promising platform for HIV prevention and treatment.

Similar as other nanoparticle-based neutralization systems and neutralizing antibodies, the HIV–TNP complexes are expected to be eliminated by the reticuloendothelial system.[25,43] While promising results are present in this initial study, we envision that toward future development, nanoparticle sizes and other properties need to be further tailored by balancing TNP pharmacokinetic profile and viral binding efficiency in vivo for maximum outcome. We also acknowledge that in current T cell membrane preparation process, extracellular vesicles in the fetal bovine serum (FBS) might potentially bind and fuse with T cell membranes, and thus alter the biological profile of T cell membranes and their functions.[44] This limitation could be addressed in the future by using serum-starved SUP-T1 cells with minimal incorporation of serum-derived extracellular vesicles.[45] In addition, for clinical translation, it is critical to meet the needs of T cell membranes. In this aspect, recent advances in methods of ex vivo cell expansion may address the large quantity of cell membrane materials demanded for clinical studies.[46] Mean-while, genetic engineering aimed at modifying primary human cells as well as cell membrane hybridization strategy may help to reduce risks of immunogenicity.[47,48] These technological breakthroughs together offer a promising prospect for translating the TNP platform and cell membrane coating technology in general.

In conclusion, we successfully derived CD4^{+} T cell membranes and fabricated TNPs, which preserve intrinsic surface markers and functions of the source cells. Specifically, the TNPs present human CD4 receptor and CCR5 or CXCR4 coreceptor with native conformation on the particle surface. Using two distinct HIV strains, X4 strain and R5 strain, it was demonstrated that the TNPs selectively bound with HIV envelop glycoprotein gp120 and effectively inhibited gp120-induced apoptosis of CD4^{+} T cells. Furthermore, the TNPs were shown to effectively neutralize both strains of HIV viruses and inhibited viral infection of

human peripheral mononuclear blood cells. Overall, the CD4$^+$ T cell membrane coating technology represents a new and attractive nanodecoy strategy for the treatment and prevention of HIV infection. This work also opens the door to using source cell-membrane-coated nanoparticles to attenuate viral infectivity in general.

Experimental Section

CD4+ T Cell Membrane Derivation:

SUP-T1 cells, a human T lymphoblast cell line (American Type Culture Collection), were cultured in the RPMI 1640 medium (Gibco) supplemented with 10% fetal bovine serum (Hyclone) and 1% penicillin−streptomycin (Gibco) in suspension flasks. To harvest the cells, suspensions were collected and centrifuged at $700 \times g$ for 5 min. After centrifugation, the supernatant was discarded, and the pellets were washed 3 times with 1× phosphate buffered saline. Then cell pellets were dispersed in an isolation buffer solution consisting of 15 mL 1× PBS, 0.5×10^{-3} M ethylene glycol-bis(2-aminoethylether)-*N,N,N′,N′*-tetraacetic acid (EGTA; Sigma), and 50 μL phosphatase inhibitor and protease inhibitor cocktails (100×, Sigma). The suspension was loaded into a dounce homogenizer and the cells were disrupted with 15 passes. Following the disruption, the suspension was spun down at $800 \times g$ for 5 min to remove large debris. The supernatant was collected and centrifuged again at 10 000 $\times g$ for 25 min, after which the pellet was discarded, and the supernatant was centrifuged at 150 000 $\times g$ for 35 min. After the centrifugation, the supernatant was discarded, and the plasma membrane was collected as an off-white pellet. The membrane pellet was then washed once with 1×10^{-3} M ethylenediaminetetraacetic acid (EDTA; USB Corporation) in H$_2$O, resuspended with gentle sonication for subsequent experiments. Membrane protein content was quantified with a Pierce BCA assay (Life Technology).

Preparation and Characterization of T-Cell-Membrane-Coated Nanoparticles (TNPs):

TNPs were fabricated using a two-step process. First, polymeric nanoparticle cores were prepared using poly(DL-lactide-*co*-glycolide) (carboxyl acid–terminated, 0.67 dL g^{-1}, 50:50, LACTEL Absorbable Polymers) through a nanoprecipitation process. The PLGA polymer was first dissolved in acetone at a concentration of 10 mg mL^{-1}. Then 1 mL of the solution was added rapidly to 4 mL of water. The nanoparticle solution was then stirred in open air for 2 h to remove the organic solvent. Fluorescently labeled nanoparticles were fabricated by incorporating 1,1′-dioctadecyl-3,3,3′,3′-tetramethylindodicarbocyanine and 4-chlorobenzenesulfonate salt (DiD; Biotium) with PLGA at 0.1 wt% during the synthesis of the cores. Second, the collected T cell membranes were mixed with nanoparticle cores at a membrane protein-to-polymer weight ratio of 1:1. The mixture was sonicated with a Fisher Scientific FS30D bath sonicator at a frequency of 42 kHz and a power of 100 W for 3 min. Nanoparticles were measured for size and size distribution with dynamic light scattering (ZEN 3600 Zetasizer, Malvern). All measurements were performed in triplicate at room temperature. Serum and PBS stabilities were studied by mixing 1 mg mL^{-1} of TNPs in water with 100% FBS and 2× PBS, respectively, at a 1:1 volume ratio. Membrane coating was confirmed with transmission electron microscopy. Briefly, 2 μL of nanoparticle suspension (1 mg mL^{-1}) was deposited onto a glow-discharged carbon-coated copper grid. Five minutes after the sample was deposited, the grid was rinsed in distilled water, followed

by staining with a drop of 1 wt% uranyl acetate. The grid was subsequently dried and visualized using a Zeiss Libra 120 PLUS EF-TEM transmission electron microscope.

Characterization of Membrane Proteins:

Protein profiles of cell lysate, cell membranes, and TNPs were characterized with sodium dodecyl sulfate polyacrylamide gel electrophoresis. Specifically, samples were prepared at a protein concentration of 0.75 mg mL^{-1} in lithium dodecyl sulfate (LDS) loading buffer (Invitrogen), heated at 80 °C for 20 min, and then loaded into Bolt 4–12% Bis−Tris Plus Gels (Invitrogen). Electrophoresis was carried out in the MOPS buffer system (Invitrogen) with an XCell SureLock Electrophoresis System (Invitrogen) per manufacturer's instruction. Following the electrophoresis, the gel was immersed in SimplyBlue buffer (Invitrogen) for 1 h to stain the proteins. To confirm the presence of CD4, CXCR4, and CCR5, the protein was transferred onto Nitrocellulose membranes (Whatman) in NuPAGE transfer buffer (Invitrogen). The membranes were blocked for 1 h and then probed with anti-CD4 (Biolegend), anti-CXCR4 (Abcam), and anti-CCR5 (Abcam), respectively. Corresponding IgG-horseradish peroxidase (HRP) conjugates were used for the secondary staining (Biolegend). Films were developed with the ECL western blotting substrate (Pierce) on a Mini-Medical/90 Developer (ImageWorks). To stain the surface proteins for membrane orientation, TNPs (100 μL, 0.5 mg mL^{-1} protein concentration) or T cells (100 μL, ≈2.5 × 10^6 cells) were blocked in 1% BSA for 30 min, followed by incubation with 0.1 μg fluorescein isothiocyanate (FITC)-labeled anti-CCR5 antibody (HEK/1/85a, Abcam) for 30 min. To remove unbound antibodies, T cell samples were spun at 4000 × g for 5 min, whereas TNP samples were centrifuged in Nanosep tubes with a molecular weight cutoff of 300 kDa and a speed of 6000 × g for 2 min. The fluorescence intensity of the unbound antibody was measured and used to calculate the amount of antibodies that bound to the TNPs or T cells.

Preparation of RBC-Membrane-Coated Nanoparticles and Poly(ethylene glycol)-Coated Nanoparticles:

RBC-membrane-coated nanoparticles were prepared by a previously reported method.[23] RBC-membrane-derived vesicles collected from male ICR mouse RBCs through hypotonic lysis were coated onto preformed PLGA cores by sonication. PEG-NPs were fabricated using a modified nanoprecipitation process. Briefly, 1 mg of 1,2-distearoyl-snglycero-3-phosphoethanolamine -N-[methoxy(poly(ethylene glycol))-2000] (DSPE-PEG2000; Avanti Polar Lipids) dissolved in chloroform was deposited in a glass vial. After organic solvent evaporation, the resulting thin film was hydrated in 1 mL water. 1 mL PLGA dissolved at 5 mg mL^{-1} in acetonitrile was added to the above aqueous phase followed by evaporation.

Specific Binding of TNPs with HIV gp120:

Recombinant HIV-1 gp120 proteins were obtained from NIH AIDS Reagent Program. Stock protein solution was diluted with 1× PBS containing 4% w/v normal goat serum, 0.5% v/v Tween-20, and 0.05% w/w sodium azide to a final concentration of 1 μg mL^{-1}. 200 μL protein solution was then added to each well of 96-well plates and incubated at 4 °C overnight for coating. Following the incubation, protein solution was removed and the wells were washed with 1× PBS. To study binding, plates were incubated with DiD-labeled TNPs

at concentrations of 0.01, 0.10, 0.25, 0.50, 1.00, and 1.80 mg mL^{-1} for 2 h at room temperature. RBC-NPs and PEG-NPs (1 mg mL^{-1}) were used as two control groups. In binding capacity and neutralization experiments, equivalent amounts (PLGA weight) of TNPs, RBC-NPs, and PEG-NPs were used. Afterward, the plates were rinsed with 1× PBS for 3 times, the fluorescent intensity was measured using SpectraMax M microplate reader (Molecular Device).

Isolation of Peripheral Blood Mononuclear Cells and Human Naive CD4+ T cells:

HIV seronegative blood buffy coat was obtained from the San Diego Blood Bank (approved by the Human Research Protections Program of the University of California San Diego). PBMCs were isolated with Ficoll-Paque PLUS (GE Healthcare) through density gradient centrifugation. Human naive CD4$^+$ T cells were purified from isolated PBMCs using negative magnetic bead selection (Miltenyl Biotec Inc). Freshly isolated PBMCs were activated by 10 μg mL^{-1} phytohemagglutinin (PHA, Sigma-Aldrich) and 25 U mL^{-1} interleukin-2 (IL-2, Roche Diagnostics) for 24 h. The activated PBMCs and isolated naive CD4$^+$ T cells were cultured in the RPMI 1640 medium within 10% FBS and 5 U mL^{-1} recombinant human IL-2 in a 5% CO$_2$ cell culture incubator at 37 °C.

Culture of Human-Monocyte-Derived Macrophages:

The isolated human PBMCs were seeded in 24-well plates in culture at 37 °C incubator with 5% CO$_2$. Nonadherent cells were removed by PBS wash. The remaining adherent cells were cultured in the RPMI 1640 medium with 10% of FBS, 1% of penicillin/streptomycin, and 10 ng mL^{-1} of macrophage colony-stimulating factor 1 (MCSF1) for additional 10 days.

TNP Inhibition of HIV-1 gp120-Induced Killing of Bystander T Cells:

To determine the ability of TNPs to inhibit HIV-1 gp120-induced killing of bystander T cells, HIV-1gp120 proteins (10 μg mL^{-1}) were incubated with 1 mg mL^{-1} of TNPs, RBC-NPs, or PEG-NPs at room temperature for 2 h. After the incubation, nanoparticle-protein mixture was added to human naive CD4$^+$ T cells with a final nanoparticle concentration of 0.1 mg mL^{-1} and a final gp120 concentration of 1 μg mL^{-1}. Treated cells were incubated at 37 °C for 24 h and then stained with 0.4% trypan blue for cell viability quantification.

HIV Neutralization with TNPs:

To study HIV–TNP binding, free viruses ($\approx 2 \times 10^6$ viruses) and viruses mixed with TNPs in water (5×10^{-7} mg mL^{-1}) were measured for size and surface zeta potential with DLS. HIV neutralization was measured using a modified protocol from Dr. David C. Montefiori. Briefly, TNPs, RBC-NPs, and PEG-NPs were dissolved in PBS. Rabbit antihuman CCR5 (GeneTEX), Rabbit antihuman CXCR4, and mouse antihuman CD4 (BioLegend) antibodies were used as antagonists to prevent binding interaction between HIVgp120 and TNPs. TNP (3.60 mg mL^{-1}) and PBS were premixed with anti-CCR5 (2 μg mL^{-1}), anti-CXCR4 (10 μg mL^{-1}), and anti-CD4 (2 μg mL^{-1}) antibodies for 1 h at 37 °C. Next, HIV-1$_{NL4-3}$ and HIV-1$_{BaL}$ (200 TCID50) were incubated with different concentrations of TNPs (0.12, 0.25, 0. 50, 1.00, 2.00, and 3.60 mg mL^{-1}), mixture of TNPs (3.60 mg mL^{-1}) and antagonist antibodies, and mixture of PBS and antagonist antibodies (3.60 mg mL^{-1} RBC-NPs or PEG-

NPs for 1 h at 37 °C). Next, all pretreated HIV was incubated with PHA- and IL-2-activated PBMCs (0.5 million cells per well), or MCSF-activated human MDMs (0.1 million cells per well) for 4 h in 96-well plates. After washing with PBS for 3 times, the PBMCs and MDMs were cultured for another 48 hf in fresh media. The supernatants were collected and subjected to measurement of HIV-1p24 production using Alliance HIV-1 p24 Antigen ELISA Kit (PerkinElmer).

Evaluation of TNP-Induced Cytotoxicity:

The collected cell culture supernatants in the above HIV neutralization study were also used to evaluate the cytotoxicity of different nanoformulations using lactate dehydrogenase cytotoxicity detection kit (TaKaRa) according to the manufacturer's protocol. The collected cell culture supernatants were loaded into 96-well plates with 100 μL per well, and further mixed with LDH reaction solutions 100 μL per well for 30 min. The reporter signal was detected using a BioTek microplate reader at an absorbance wavelength of 490 nm (BioTek).

Statistical Analysis:

DLS and plate reader data represent averaged values (obtained from three replicates) with standard deviation shown as error bars. For photographs of SDS-PAGE and Western blot studies, the experiments were performed in triplicate and a representative image was shown. For examining the statistical significance, unpaired two-tailed t-tests were performed in GraphPad Prism 7 with confidence level $P < 0.05$ deemed significant.

Acknowledgements

References

[1]. Finzi D, Blankson J, Siliciano JD, Margolick JB, Chadwick K, Pierson T, Smith K, Lisziewicz J, Lori F, Flexner C, Quinn TC, Chaisson RE, Rosenberg E, Walker B, Gange S, Gallant J, Siliciano RF, Nat. Med 1999, 5, 512. [PubMed: 10229227]

[2]. Perreau M, Banga R, Pantaleo G, Trends Mol. Med 2017, 23, 945. [PubMed: 28890135]

[3]. Campbell EM, Hope TJ, Nat. Rev. Microbiol 2015, 13, 471. [PubMed: 26179359]

[4]. Hatano H, Delwart EL, Norris PJ, Lee TH, Neilands TB, Kelley CF, Hunt PW, Hoh R, Linnen JM, Martin JN, Busch MP, Deeks SG, AIDS 2010, 24, 2528.

[5]. Dahabieh MS, Battivelli E, Verdin E, Annu. Rev. Med 2015, 66, 407. [PubMed: 25587657]

[6]. Harrigan PR, Whaley M, Montaner JSG, AIDS 1999, 13, F59. [PubMed: 10371167]

[7]. Garcia F, Plana M, Vidal C, Cruceta A, O'Brien WA, Pantaleo G, Pumarola T, Gallart T, Miro JM, Gatell JM, AIDS 1999, 13, F79. [PubMed: 10449278]

[8]. Anstett K, Brenner B, Mesplede T, Wainberg MA, Retrovirology 2017, 14, 36. [PubMed: 28583191]

[9]. Beyrer C, Pozniak A, New Engl. J. Med 2017, 377, 1605. [PubMed: 29069566]

[10]. Xu L, Pegu A, Rao E, Doria-Rose N, Beninga J, McKee K, Lord DM, Wei RR, Deng GJ, Louder M, Schmidt SD, Mankoff Z, Wu L, Asokan M, Beil C, Lange C, Leuschner WD, Kruip J, Sendak R, Do Kwon Y, Zhou TQ, Chen XJ, Bailer RT, Wang KY, Choe M, Tartaglia LJ, Barouch DH, O'Dell S, Todd JP, Burton DR, Roederer M, Connors M, Koup RA, Kwong PD, Yang ZY, Mascola JR, Nabel GJ, Science 2017, 358, 85. [PubMed: 28931639]

[11]. McCoy LE, Burton DR, Immunol. Rev 2017, 275, 11. [PubMed: 28133814]

[12]. Lewis GK, Pazgier M, DeVico AL, Immunol. Rev 2017, 275, 271. [PubMed: 28133809]

[13]. Wijesundara DK, Ranasinghe C, Grubor-Bauk B, Gowans EJ, Front. Microbiol 2017, 8, 2091. [PubMed: 29118747]

[14]. Stephenson KE, D'Couto HT, Barouch DH, Curr. Opin. Immunol 2016, 41, 39. [PubMed: 27268856]

[15]. Mamo T, Moseman EA, Kolishetti N, Morales CS, Shi J, Kuritzkes DR, Langer R, von Andrian U, Farokhzad OC, Nano-medicine 2010, 5, 269.

[16]. Glass JJ, Kent SJ, De Rose R, Expert Rev. Vaccines 2016, 15, 719. [PubMed: 26783186]

[17]. das Neves J, Nunes R, Rodrigues F, Sarmento B, Adv. Drug Delivery Rev 2016, 103, 57.

[18]. Ramana LN, Anand AR, Sethuraman S, Krishnan UM, J. Controlled Release 2014, 192, 271.

[19]. Friedman SH, Decamp DL, Sijbesma RP, Srdanov G, Wudl F, Kenyon GL, J. Am. Chem. Soc 1993, 115, 6506.

[20]. Bowman MC, Ballard TE, Ackerson CJ, Feldheim DL, Margolis DM, Melander C, J. Am. Chem. Soc 2008, 130, 6896. [PubMed: 18473457]

[21]. Adesina SK, Akala EO, Mol. Pharmaceutics 2015, 12, 4175.

[22]. Mishra V, Kesharwani P, Jain NK, Drug Discovery Today 2014, 19, 1913. [PubMed: 25281591]

[23]. Hu CMJ, Zhang L, Aryal S, Cheung C, Fang RH, Zhang L, Proc. Natl. Acad. Sci. USA 2011, 108, 10980. [PubMed: 21690347]

[24]. Fang R, Kroll A, Gao W, Zhang L, Adv. Mater 2018, 30, 1706759.

[25]. Hu CMJ, Fang RH, Copp J, Luk BT, Zhang L, Nat. Nanotechnol 2013, 8, 336. [PubMed: 23584215]

[26]. Hu CMJ, Fang RH, Luk BT, Zhang L, Nat. Nanotechnol 2013, 8, 933. [PubMed: 24292514]

[27]. Copp JA, Fang RH, Luk BT, Hu CMJ, Gao W, Zhang K, Zhang L, Proc. Natl. Acad. Sci. USA 2014, 111, 13481. [PubMed: 25197051]

[28]. Thamphiwatana S, Angsantikul P, Escajadillo T, Zhang QZ, Olson J, Luk BT, Zhang S, Fang RH, Gao W, Nizet V, Zhang L, Proc. Natl. Acad. Sci. USA 2017, 114, 11488. [PubMed: 29073076]

[29]. Freed EO, Nat. Rev. Microbiol 2015, 13, 484. [PubMed: 26119571]

[30]. Fang RH, Hu CMJ, Luk BT, Gao W, Copp JA, Tai YY, O'Connor DE, Zhang L, Nano Lett 2014, 14, 2181. [PubMed: 24673373]

[31]. Luk BT, Hu CMJ, Fang RNH, Dehaini D, Carpenter C, Gao W, Zhang L, Nanoscale 2014, 6, 2730. [PubMed: 24463706]

[32]. Tassa C, Duffner JL, Lewis TA, Weissleder R, Schreiber SL, Koehler AN, Shaw SY, Bioconjugate Chem 2010, 21, 14.

[33]. Garg H, Mohl J, Joshi A, Viruses 2012, 4, 3020. [PubMed: 23202514]

[34]. Gobeil LA, Lodge R, Tremblay MJ, J. Virol 2013, 87, 735. [PubMed: 23115275]

[35]. Carter GC, Bernstone L, Baskaran D, James W, Virology 2011, 409, 234. [PubMed: 21056892]

[36]. Marechal V, Prevost MC, Petit C, Perret E, Heard JM, Schwartz O, J. Virol 2001, 75, 11166. [PubMed: 11602756]

[37]. Clavel F, Hance AJ, New Engl. J. Med 2004, 350, 1023. [PubMed: 14999114]

[38]. Kulkarni AA, Fuller C, Korman H, Weiss AA, Iyer SS, Bioconju-gate Chem 2010, 21, 1486.

[39]. Hendricks GL, Weirich KL, Viswanathan K, Li J, Shriver ZH, Ashour J, Ploegh HL, Kurt-Jones EA, Fygenson DK, Finberg RW, Comolli JC, Wang JP, J. Biol. Chem 2013, 288, 8061. [PubMed: 23362274]

[40]. Yang T, Ke HT, Wang QL, Tang YA, Deng YB, Yang H, Yang XL, Yang P, Ling DS, Chen CY, Zhao YL, Wu H, Chen HB, ACS Nano 2017, 11, 10012. [PubMed: 28945969]

[41]. Yang T, Liu L, Deng YB, Guo ZQ, Zhang GB, Ge ZS, Ke HT, Chen HB, Adv. Mater 2017, 29, 1700487.

[42]. He H, Ji SS, He Y, Zhu AJ, Zou YL, Deng YB, Ke HT, Yang H, Zhao YL, Guo ZQ, Chen HB, Adv. Mater 2017, 29, 1606690.

[43]. Halma C, Daha MR, Vanes LA, Clin. Exp. Immunol 1992, 89, 1. [PubMed: 1628416]

[44]. Mokarizadeh A, Delirezh N, Morshedi A, Mosayebi G, Farshid AA, Dalir-Naghadeh B, Vet. Res. Forum 2012, 3, 257. [PubMed: 25653768]

[45]. Yang XY, Gabuzda D, J. Virol 1999, 73, 3460. [PubMed: 10074203]

[46]. Rasmussen AM, Borelli G, Hoel HJ, Lislerud K, Gaudernack G, Kvalheim G, Aarvak T, Immunol J. Methods 2010, 355, 52.

[47]. Zhang L, Morgan RA, Adv. Drug Delivery Rev 2012, 64, 756.

[48]. Dehaini D, Wei XL, Fang RH, Masson S, Angsantikul P, Luk BT, Zhang Y, Ying M, Jiang Y, Kroll AV, Gao W, Zhang L, Adv. Mater 2017, 29, 1606209.
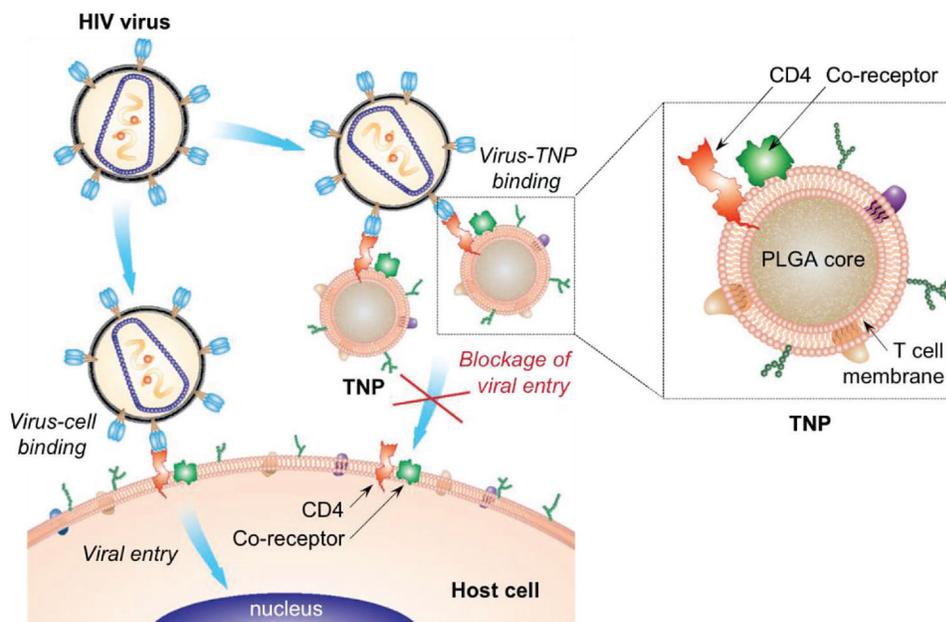
Figure 1.
Schematic representation of T-cell-membrane-coated nanoparticles (denoted as "TNPs") designed for attenuating HIV infectivity. TNPs were constructed by wrapping polymeric cores with natural CD4⁺ T cell membranes, which contain key antigens including CD4 receptor and CCR5 or CXCR4 coreceptors for viral targeting. By replicating the surface antigen profile of source T cells, TNPs can act as decoys to bind with T cell targeted viruses and subsequently block viral entry into and infection of the target cells.
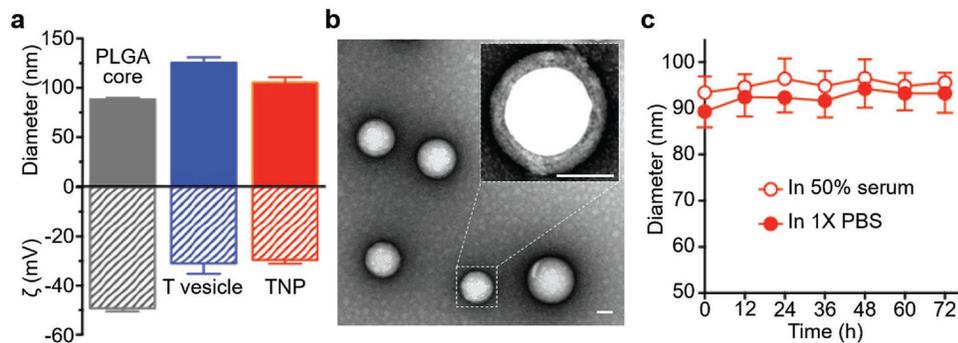
Figure 2.
Physicochemical characterization of TNPs. a) Dynamic light scattering measurements of hydrodynamic size (diameter, nm) and surface zeta potential (ζ, mV) of PLGA cores, T-cell-membrane-derived vesicles (T vesicles), and TNPs. Error bars represent standard deviations ($n = 3$). b) Transmission electron microscopy images of TNPs negatively stained with uranyl acetate. Scale bar = 50 nm. Inset: A zoomed-in view of a single TNP. Scale bare = 50 nm. c) Stability of TNPs in 1× PBS or 50% fetal bovine serum, determined by monitoring particle size (diameter, nm), over a span of 72 h. Error bars represent standard deviations ($n = 3$).
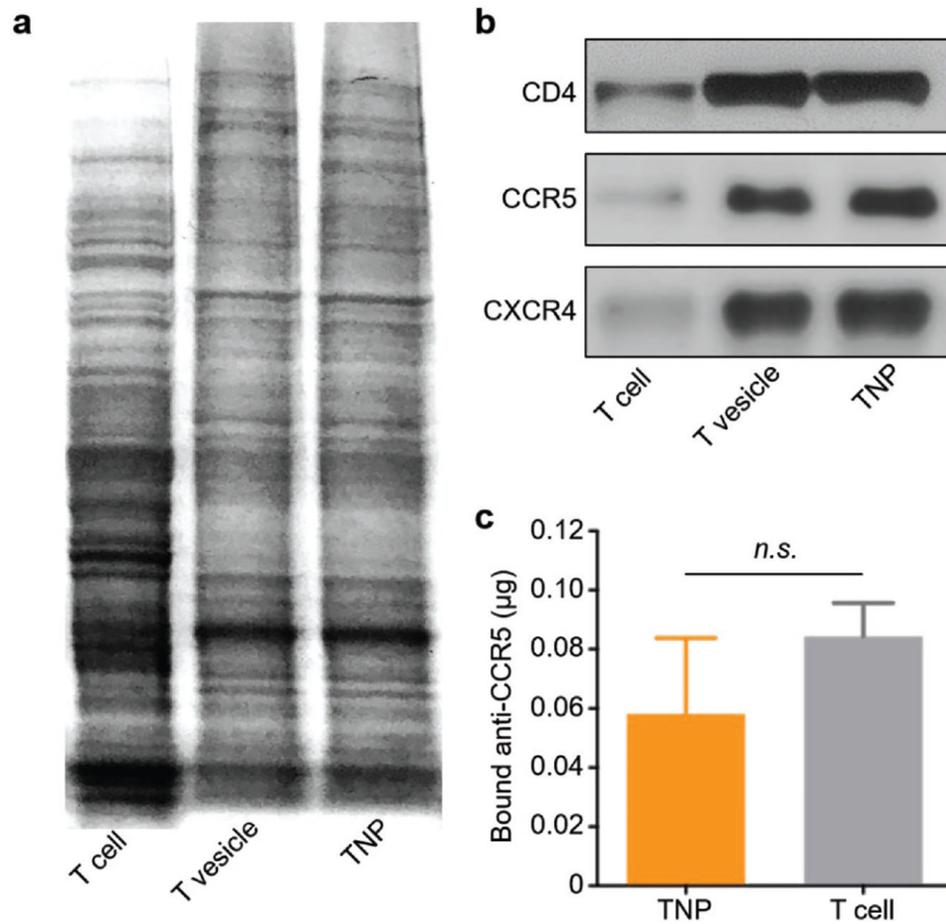
Figure 3.
Characterization of TNP membrane proteins. a) SDS-PAGE protein analysis of T cell lysate, T vesicles, and TNPs. Samples were run at equivalent protein concentrations and stained with Coomassie Blue. b) Western blotting analysis for CD4 receptor, and CCR5 and CXCR4 coreceptors related to HIV binding. c) Comparison of the fluorescence intensity measured from TNPs (100 μL, 0.5 mg mL^{-1} protein concentration) or T cells (100 μL, $\approx 2.5 \times 10^6$ cells) containing equal amounts of membrane content and stained with fluorescein-isothiocyanate-labeled CCR5 antibodies. Error bars represent standard deviations (n.s.: not significant).
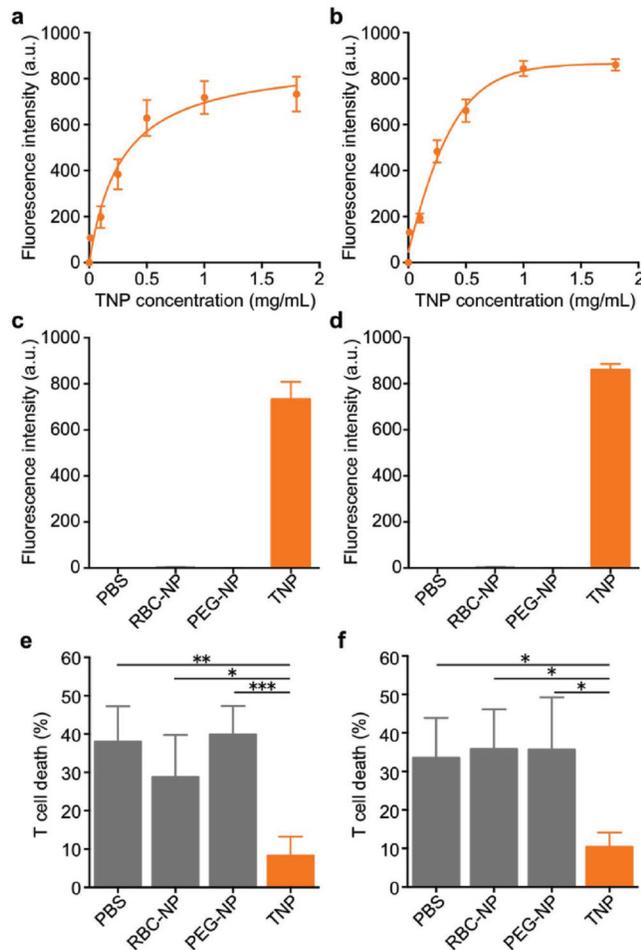
Figure 4.
TNP binding capacity and specificity against HIV envelope glycoprotein gp120. In addition to TNPs, RBC-membrane-coated nano-particle and pegylated polymeric nanoparticle (PEG-NP) and PBS were used as control groups. a) Binding capacity of TNPs with gp120$_{IIIB}$. b) Binding capacity of TNPs with gp120$_{BaL}$. c) Binding specificity of TNPs with gp120$_{IIIB}$. d) Binding specificity of TNPs with gp120$_{BaL}$. e) TNP neutralization against bystander T cell killing induced by gp120$_{IIIB}$. f) TNP neutralization against bystander T cell killing induced with gp120$_{BaL}$. Data shown as mean ± SD of triplicate wells and are representative of two independent experiments. $*p < 0.05$, $**p < 0.01$, $***p < 0.001$.
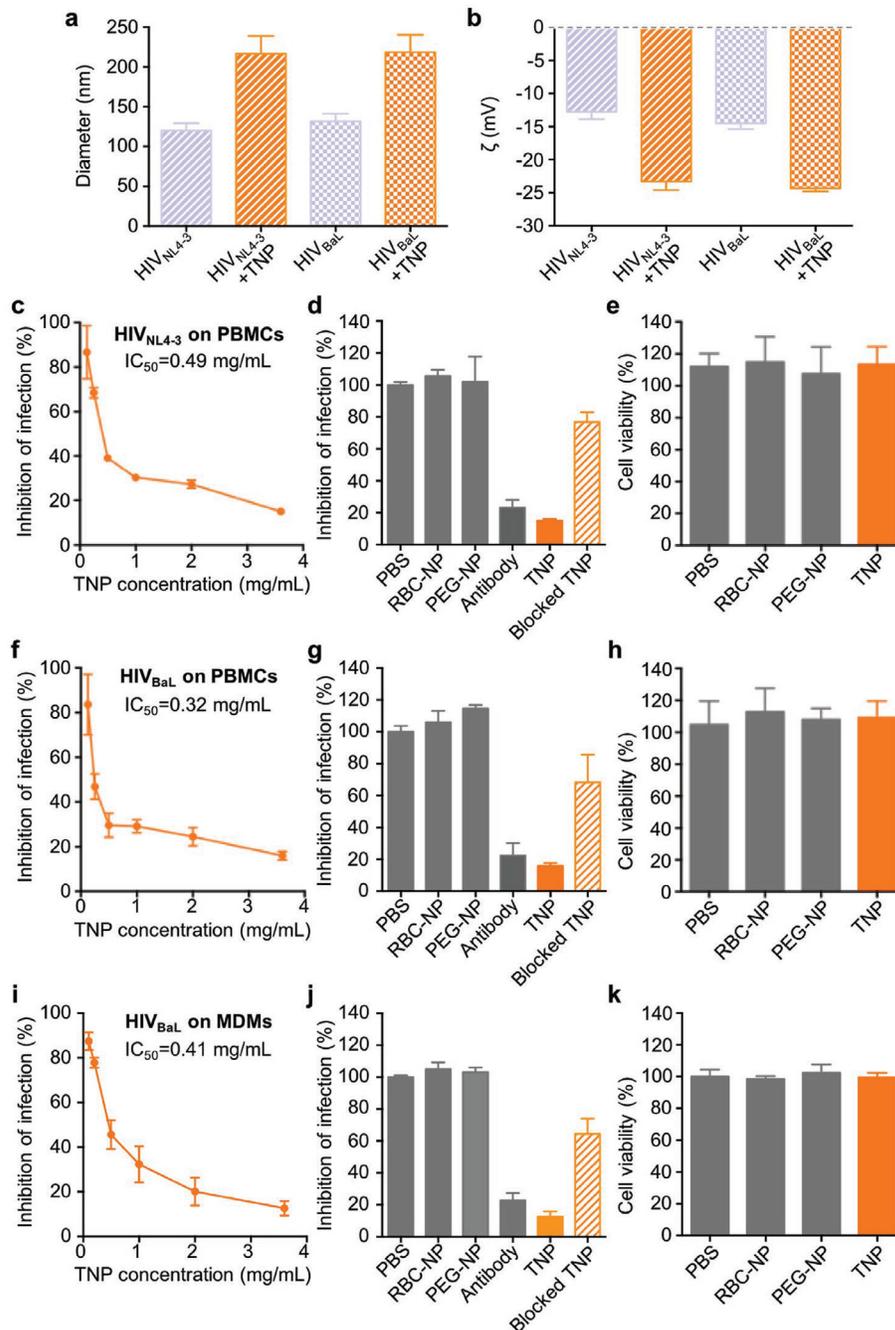
Figure 5.
TNPs neutralizing HIV infectivity. a) Hydrodynamic size (diameter, nm) and b) surface zeta potential (ζ, mV) of HIV viruses and HIV–TNP complexes measured by dynamic light scattering. Error bars represent standard deviations (n = 3). The inhibition of HIV infection by TNPs was tested with two viral strains on peripheral blood mononuclear cells or human-monocyte-derived macrophages. c–e) HIV_{NL4-3} strain on PBMCs, f–h) HIV_{BaL} strain on PBMCs, and i–k) HIV_{BaL} strain on MDMs. c,f,i) Inhibition of viral infection was tested with various TNP concentrations on each strain. d,g,j) Inhibition specificity was examined by

comparing the inhibition of infection with TNPs, RBC-NPs, PEG-NPs, antibodies (a mixture of anti-CCR5, anti-CXCR4, and anti-CD4 antibody at final concentrations of 2, 5, and 2 μg mL^{-1}, respectively), and TNP blocked with the antibody mixture, respectively. e,h,k) Cell viability was compared among TNPs, RBC-NPs, and PEG-NPs, respectively, to confirm that inhibition of infection was not due to vehicle-induced cytotoxicity. Data shown as mean ± SD of triplicate wells and are representative of two independent experiments.